

1 *Supplementary Materials*

2 **Synthesis, Physical, Mechanical and Antibacterial** 3 **Properties of Nanocomposites based on Poly(vinyl** 4 **alcohol)/Graphene Oxide–Silver Nanoparticles**

5 **Mónica Cobos**¹, **Iker De-La-Pinta**², **Guillermo Quindós**², **M. Jesús Fernández**¹, **M. Dolores**
6 **Fernández**^{1,*}

7 ¹ Department of Polymer Science and Technology, Faculty of Chemistry, University of the Basque Country
8 (UPV/EHU), Paseo Manuel Lardizábal 3, 20018 San Sebastián, Spain; monica.cobos@ehu.es
9 (M.C.); mjesus.fernandez@ehu.es (M.J.F.)

10 ² Department of Immunology, Microbiology and Parasitology, Faculty of Medicine and Nursing, University
11 of the Basque Country (UPV/EHU), Barrio Sarriena s/n, Leioa 48940, Spain; iker.delapinta@ehu.es
12 (I.D.L.P.); guillermo.quindos@ehu.es (G.Q.)

13 * Correspondence: mariadolores.fernandez@ehu.es (M.D.F.); Tel.: +34-943-01-8179
14

15 *Preparation of Graphene Oxide (GO)*

16 A flask containing a mixture of 2 g graphite, 50 mL H₂SO₄ and 1 g NaNO₃ was placed in a water
17 bath at 0 °C. Then, 6 g of KMnO₄ was slowly added, and the mixture was subsequently heated up to
18 35 °C for 1 h. After the slow addition of 100 mL of de-ionized water, 10 mL of 30% H₂O₂ was
19 incorporated into the solution. The suspension was subjected to centrifugation to separate the solid,
20 that was washed with water, HCl and finally again with water until reaching neutral pH. Finally, the
21 product, graphite oxide (GrO), was obtained by freeze-drying. GO was obtained after ultrasonication
22 of an aqueous dispersion of GrO.

23 *Physicochemical Characterization*

24 *Structure and Morphology*

25 FTIR spectra were recorded using a Thermo Nicolet iS10 spectrometer (Thermo Fisher Scientific,
26 Madison, WI, USA) equipped with an attenuated total reflectance accessory (ATR). UV-Vis spectra
27 were measured on a Perkin Elmer Lambda 25 spectrometer (Shelton, CT, USA) in the range 200–800
28 nm. Surface chemistry characterization of graphenic materials was performed by XPS on a SPECS
29 system with a monochromatic Al K α X-ray source (1486.6 eV) and a Phoibos 150 1D-DLD analyzer
30 (Berlin, Germany). The core level spectra were obtained at a photoelectron take-off angle of 90°,
31 measured with respect to the sample surface. The XPS survey-scan spectra were taken with pass
32 energy of 80 eV, 1 eV energy step, and 0.1 s dwell time. The individual high-resolution spectra were
33 acquired with pass energy of 30 eV, 0.1 eV energy step, and 0.1 s dwell time. Raman characterization
34 of GO and GO–AgNPs were carried out with a Renishaw Invia microscope (Gloucestershire, UK)
35 with laser frequency of 514 nm as an excitation source. The spectra were measured from 500 to 3500
36 cm⁻¹. XRD spectra of graphenic materials, neat PVA and PVA/GO–AgNPs nanocomposites were
37 performed using a Malvern Panalytical (Almelo, Netherlands) X'PERT PRO automatic diffractometer
38 operating at 40 kV and 40 mA, in theta-theta configuration, secondary monochromator with Cu-K α
39 radiation ($\lambda = 1.5418 \text{ \AA}$) and a PIXcel solid state detector (active length in 2θ 3.347°). Data were
40 collected from 1 to 50° 2θ for GO and PVA, and from 1 to 90° 2θ for GO–AgNPs and PVA/GO–AgNPs

41 samples (step size = 0.026° and time per step = 80 s, total time 20 min) at room temperature. A variable
42 divergence slit giving a constant 5mm area of sample illumination was used. The interlayer
43 separation in the graphenic material was calculated by the Bragg's law ($\lambda = 2d \sin\theta$). TEM
44 measurements were carried out using a Philips Tecnai G2 20 TWIN TEM instrument (Eindhoven,
45 Netherlands) at 200 kV accelerated voltage. GO–AgNPs samples were prepared by drop-coating
46 dilute suspensions onto carbon coated copper grids and dried at room temperature. PVA/GO–AgNPs
47 nanocomposites were sectioned with a Leica EM UC6 ultramicrotome apparatus and placed in coated
48 cooper grids. SEM images were also obtained for PVA and PVA/GO–AgNPs films, using a Hitachi
49 S-4800 scanning electron microscope (Tokyo, Japan) operated at 5 kV accelerating voltage. Samples
50 were fractured in liquid nitrogen and the cross-sections were sputtered with gold, after which the
51 cross-section morphology was examined.

52 *Thermal characterization*

53 Thermogravimetric analysis (TGA) and differential scanning calorimetry analyses (DSC) were
54 used for thermal characterization. TGA tests were performed on a TG-Q-500 (TA instruments, New
55 Castle, DE, USA) under nitrogen at a heating rate of 10 °C/min, from 40 to 800 °C. DSC thermograms
56 were recorded with a Mettler Toledo DSC 3+ unit (Greifensee, Switzerland), at a heating rate of
57 10°C/min under nitrogen atmosphere at a flow rate of 20 mL/min, over a temperature range of -30 to
58 250 °C.

59 *Mechanical characterization*

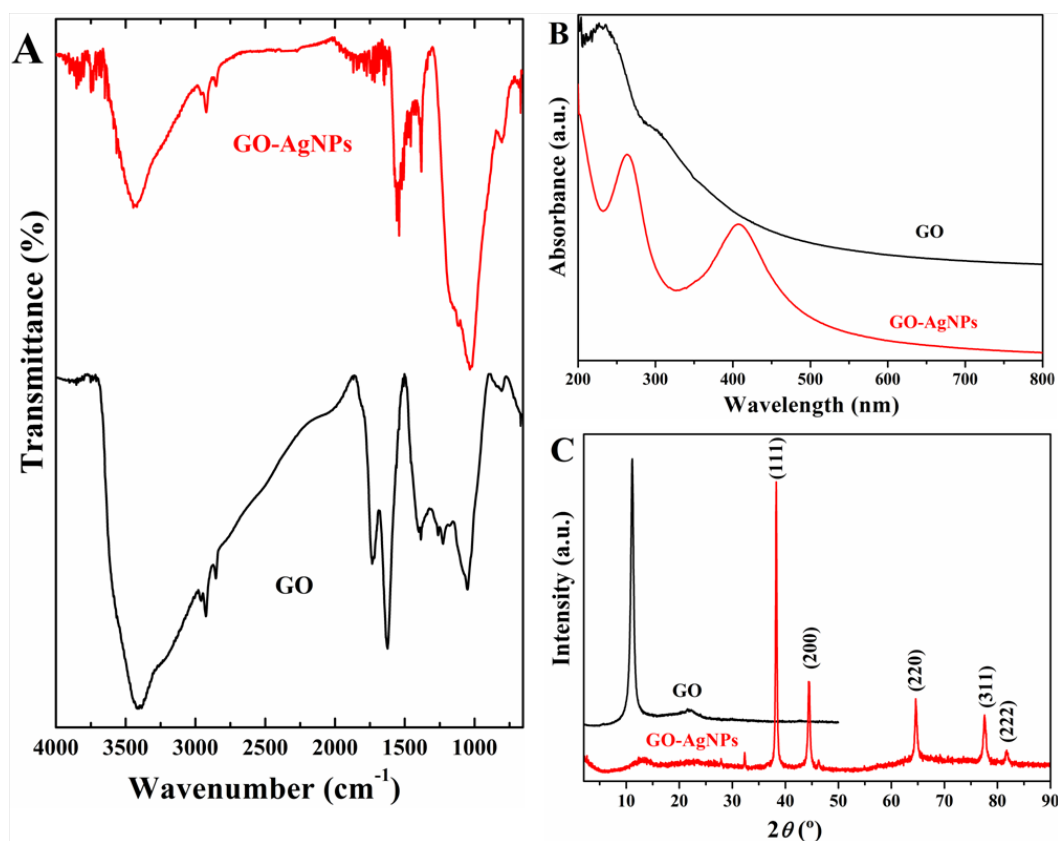
60 The mechanical characterization was conducted in an electromechanical testing machine
61 (Instron 5967, Norwood, MA, USA) with a 500 N load cell, a displacement rate of 5 mm/min, and a
62 gauge length of 10 mm. Dog-bone shaped specimens were punched out of the films, and maintained
63 at room temperature at a relative humidity of 58 % for one week prior to testing, to guarantee
64 moisture equilibrium of the specimens. Ten specimens of each sample were tested.

65 *Characterization of GO and GO–AgNPs hybrid*

66 The successful synthesis of graphene oxide (GO) and GO–AgNPs hybrid was confirmed by
67 FTIR, UV-vis, X-ray diffraction, XPS and Raman spectroscopy. Figure S1 compares FTIR, UV-vis and
68 XRD spectra of GO and GO–AgNPs hybrid. FTIR spectrum of GO shows the strong bands related to
69 the C=O carbonyl stretching vibrations of the COOH groups at 1734 cm⁻¹, located at the edges of GO
70 sheets, the bending of tertiary C-OH groups at 1362 cm⁻¹, and the stretching vibration of C-O of
71 epoxide groups at 1052 cm⁻¹ (Figure S1A). The strong band at 3800-300 cm⁻¹ is assigned to the
72 stretching vibrations of structural OH groups and physisorbed water molecules. Regarding the FTIR
73 spectrum of GO–AgNPs hybrid, the weakening of the mentioned bands can be observed, suggesting
74 the simultaneous partial reduction of GO.

75 The comparison of the UV-vis spectra of GO and GO–AgNPs shows the red shift of the GO peak
76 from 230 to 265 nm, the disappearance of the shoulder at 303 nm, and the appearance of the surface
77 plasmon resonance band of AgNPs at 404 nm, when AgNPs are incorporated on the surface of GO
78 (Figure S1B). These results confirm the partial reduction of GO and the presence of small spherical
79 shape AgNPs attached to GO surface.

80 XRD patterns of GO and GO–AgNPs are presented in Figure S1C. The XRD pattern of GO
81 exhibits 2 θ peak at 11.1°, whereas the hybrid displays peaks from 2 θ = 30° to 90°, but the peak of GO
82 is not seen. Those peaks correspond to the (111), (200), (311) and (222) planes of the face centred cubic
83 of AgNPs. All these results indicated the decoration of GO with AgNPs and the exfoliation of GO–
84 AgNPs sheets.



85

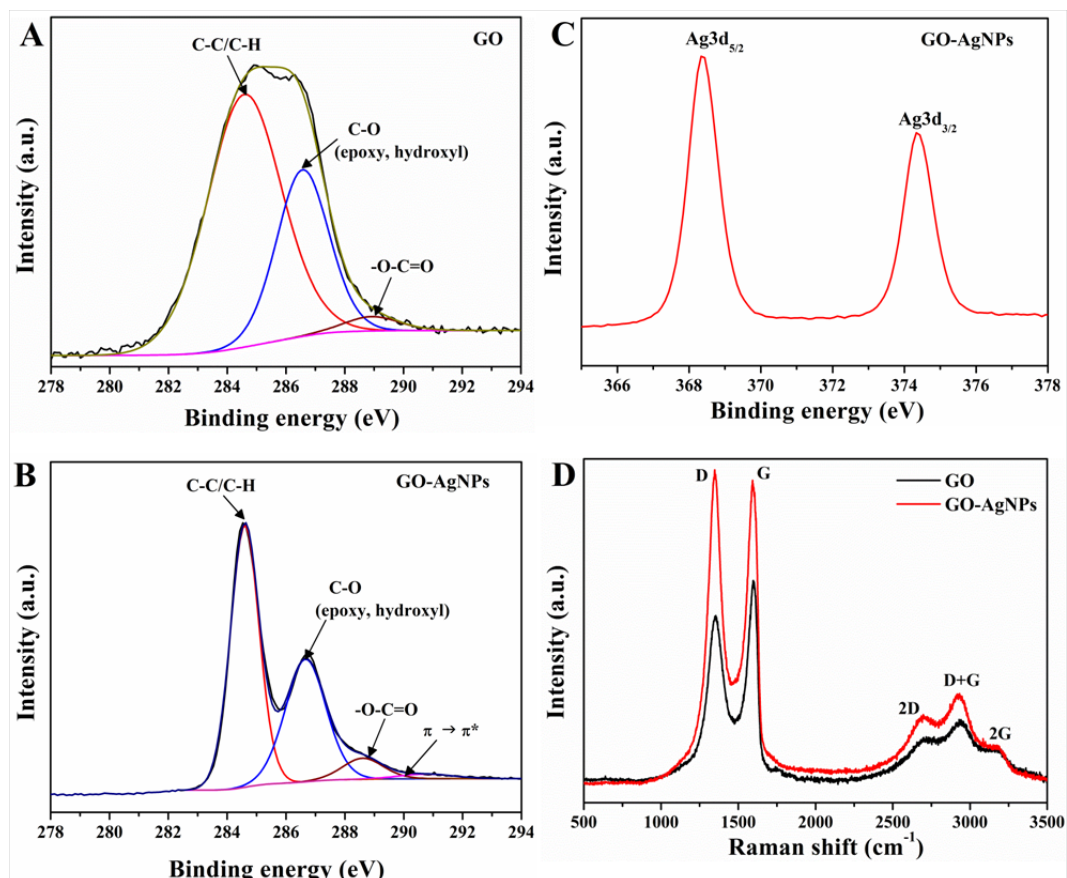
86

Figure S1. (A) FTIR, (B) UV-vis and (C) XRD spectra of GO and GO–AgNPs hybrid.

87

88 The C1s XPS spectra for GO and GO–AgNPs are shown in Figures S2A and B, respectively. The
 89 intensity of C–O peak is significantly reduced, the C–C peak narrows and the shake-up satellite at
 90 ~290 eV appears after the formation of AgNPs on the GO surface. These results confirm the
 91 simultaneous partial reduction of GO during the preparation of the hybrid. The presence of Ag3d5/2
 92 and Ag3d3/2 peaks found at 368.4 and 374.4 eV, respectively, in the Ag3d spectrum (Figure S2C)
 93 indicate the formation of metallic silver.

94 Raman spectra of GO and GO–AgNPs hybrid is provided in Figure 2D. There is a shift of all the
 95 bands to lower wavenumbers, an increase of the intensity of D band and an increase of the intensity
 96 ratio I_D/I_G after the attachment of AgNPs to the GO surface. From these results, it can be inferred that
 97 structural defects have been introduced in the graphene sheets.



98

99

100

Figure S2. C1s XPS spectrum of (A) GO and (B) GO-AgNPs; (C) Ag3d spectrum of GO-AgNPs; (D) Raman spectra of GO and GO-AgNPs.

101

102

103

104

105

106

107

108

109

110

111

112

113

114

115

116

117

118

119

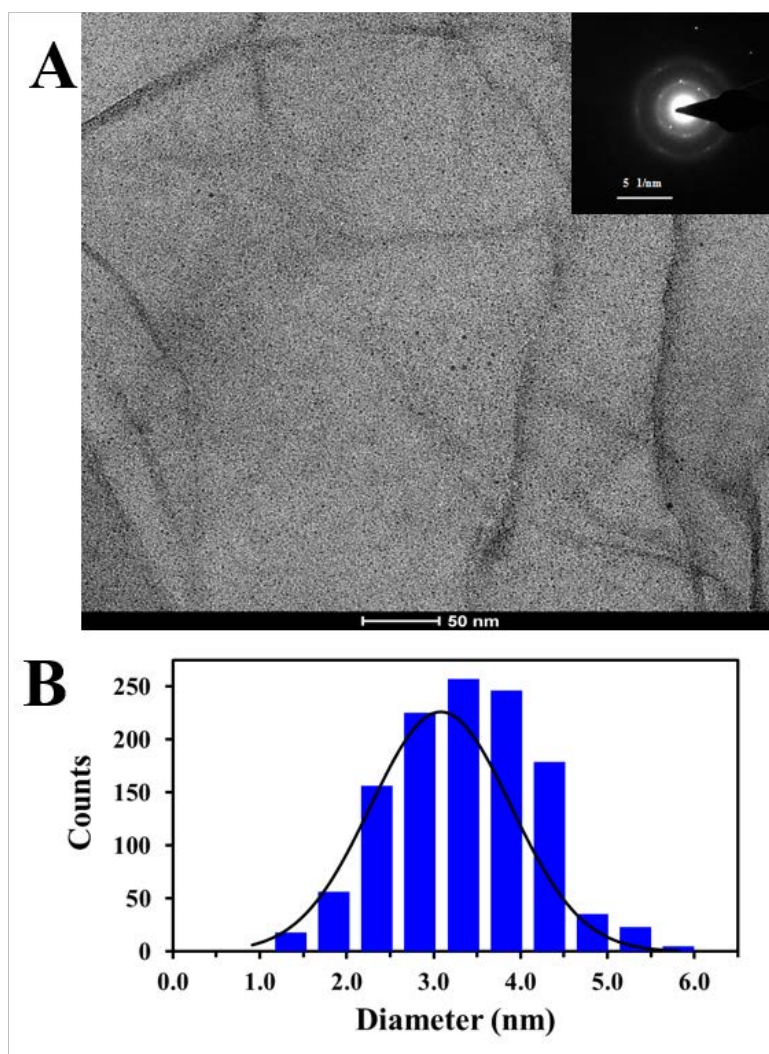
120

121

122

123

124 The morphology and structure of the GO–AgNPs hybrid was analysed by TEM. The image of
125 Figure S3A shows the spherical AgNPs, with average size of 3.1 ± 0.8 nm, distributed uniformly over
126 the surface of GO. AgNPs size was determined by measuring the diameter of 1200 nanoparticles in
127 several TEM images. The histogram shows a narrow size distribution, with most of particles under 4
128 nm in diameter (Figure S3B). The selected area electron diffraction (SAED) pattern obtained from the
129 hybrid is shown as an inset in Figure S3A. It shows the diffraction rings corresponding to (111), (200),
130 (220) and (311) of Ag, indicating the polycrystalline nature of silver.
131
132



133

134

135 **Figure S3.** (A) TEM image of GO–AgNPs hybrid, inset shows SAED pattern. (B) AgNPs size
136 distribution.

137

138

139

140

141

142

143

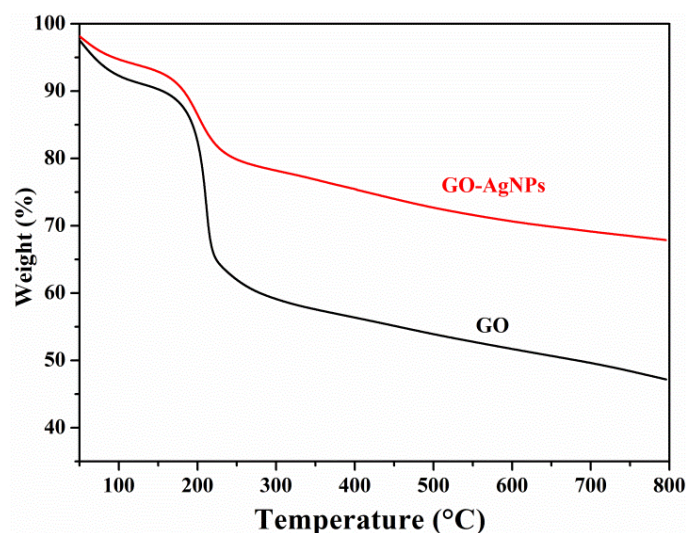
144

145

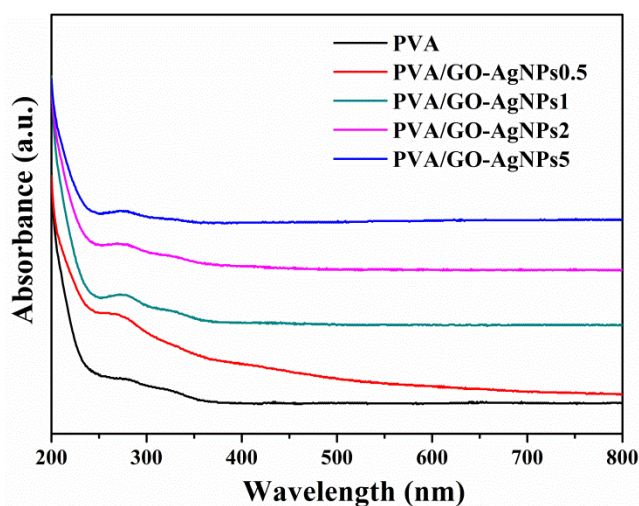
146

147 **Thermal stability of GO and GO–AgNPs hybrid**

148 Thermogravimetric analysis (TGA) was used to evaluate the thermal stability of the graphenic
149 materials. Figure S4 shows the TGA mass loss curves. Both curves show two decomposition steps,
150 the first one is located below 120 °C and the second one is found in the range 140–300 °C. The first
151 weight loss is attributed to the elimination of the interlaminar water, whereas in the second step less
152 stable oxygen containing functional groups decompose. The mass loss during this step was about
153 32% and 16% for GO and GO–AgNPs hybrid, respectively. The lower mass loss for the hybrid indicates that
154 GO was partially reduced during the synthesis process of the hybrid.
155



156
157
158 **Figure S4.** TGA curves of GO and GO–AgNPs hybrid.

159
160
161
162
163 **Lixiviation test**

164
165 **Figure S5.** UV-vis absorption spectra of leachates from PVA/GO–AgNPs
166 nanocomposite films after water immersion.
167